

Cooperative Space-Time Coded OFDM with Timing Errors and Carrier Frequency Offsets

F. Sánchez*, T. Zemen*, G. Matz[†], F. Kaltenberger[‡], N. Czik*

*FTW Telecommunications Research Center, Vienna, Austria

[†]Inst. of Communications and RF Engineering, Vienna University of Technology, Vienna, Austria

[‡]Institute Eurecom, Sophia Antipolis, France

Abstract—The use of distributed space-time codes in cooperative communications promises to increase the rate and reliability of data transmission. These gains were mostly demonstrated for ideal scenarios, where all the nodes are perfectly synchronized.

Considering a cooperative uplink scenario with asynchronous nodes, the system suffers from two effects: timing errors and individual carrier frequency offsets. In effect, timing errors can completely cancel the advantages introduced by space-time codes, while individual carrier frequency offsets provide a great challenge to receivers. Indeed, in cooperative communications, frequency offsets are perceived as a time-variant channel, even if the individual links are static.

We show that using OFDM, space-time codes (STCs) become robust to timing errors. Channel estimation and tracking takes care of frequency offsets. Our simulations demonstrate that the bit error rate (BER) performance improves by an order of magnitude, when using a cooperative system design, which takes these two effects into account.

Index Terms—OFDM, Block codes, distributed space-time code, virtual MIMO, diversity methods, cooperative systems, time-varying channels, delay effects, channel estimation, spatial diversity, transmit diversity, Slepian basis expansion.

I. INTRODUCTION

Cooperative communications can increase both data rate and link reliability. Large gains can be expected when nodes are acting as a virtual array. Popular schemes to utilize multi-node diversity are based on STCs. Many publications study the advantageous effects of STCs in distributed cooperative communications but assuming perfectly synchronized nodes, i.e. their signals have no carrier frequency offsets, and arrive at the same time at the receiver [1].

The performance of STCs is deteriorated by synchronization errors [2]. Timing offsets in the order of the duration of a symbol can destroy the code structure, if the STC is not designed to be delay tolerant. Damen *et al.* [3] and Sarkiss *et al.* [4] adapted STCs to be delay tolerant, however the authors did not investigate the effect of non-sample-spaced timing offsets. Li and Xia [5] proposed to combine space-time trellis codes with the stack construction concept from [6], but their codes require high complexity for optimal decoding.

This work was supported by the project PUCCO funded by the Vienna Science and Technology Fund (WWTF). The work was carried out within the framework of COST 2100 and in the FP7 Network of Excellence NEWCOM++. The Telecommunications Research Center Vienna (FTW) is supported by the Austrian Government and the City of Vienna within the competence center program COMET.

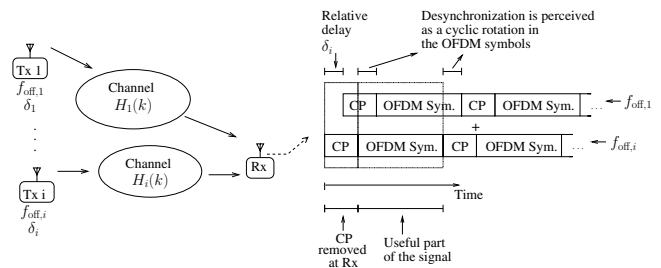


Fig. 1. OFDM distributed cooperative transmission.

Many current communication systems are based on orthogonal frequency division multiplexing (OFDM). Prominent examples are LTE [7], WiFi [8], and DVB-T [9]. DVB-T single frequency networks use distributed OFDM transmission, hence several television stations transmit simultaneously the same signal. OFDM uses the cyclic prefix (CP) to prevent inter-symbol interference. It turns out that the CP provides also the means to make cooperative communication systems inherently robust against timing synchronization errors.

In this contribution we combine OFDM with STCs and time-variant channel estimation for distributed cooperative communications scenarios. The system presented successfully compensates the main effects of real implementations i.e. timing errors and frequency offsets between the distributed nodes. We consider a scenario where at least two nodes join up to transmit a common message to a distant base station as outlined in Fig. 1. Using STCs, the nodes increase the diversity and the overall uplink SNR, leading to a lower BER.

We show that the combination of OFDM and STC is advantageous when using a proper receiver architecture. We consider two STCs: delay diversity and the Alamouti code. Carrier frequency offsets introduced by the individual transmitters (TXs) lead to an effective time-variant channel at the receiver, this effect can be compensated by proper time variant channel estimation. We employ a channel estimator based on discrete prolate spheroidal sequences (DPSs), which tracks the channel in the time-frequency domain simultaneously.

The paper is organized as follows: Sec. II discusses the system model of our cooperative communication system. Section III analyses the system impairments. In Sec. IV, we detail the channel estimators used. Simulation results are presented in Sec. V. Finally, in Sec. VI, we draw conclusions.

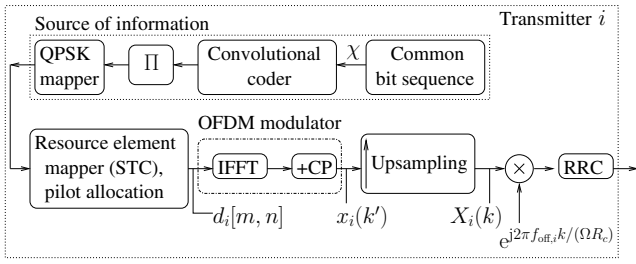


Fig. 2. TX for space-time coded OFDM distributed cooperative transmission. The source of information is the same for all nodes.

II. SYSTEM MODEL

The system model describes the cooperative space-time coded transmission from multiple OFDM TXs to the receiver. In practical scenarios, relay nodes may assist a common source. In our work we assume that these cooperating nodes have received the data from the source beforehand.

A. OFDM for distributed cooperative transmission

We consider the equalization and detection problem for an OFDM link [10]. The OFDM system utilizes N subcarriers and a CP with length G . The transmission is block-oriented with block length M , uses a bandwidth B and the sampling rate at the receiver side is $R_C = 1/T_C = B$. The OFDM symbol duration is given by $T_S = (N + G)T_C$ and the subcarrier frequency spacing is $1/(T_C N)$.

1) *Transmitters*: Fig. 2 shows the block diagram for cooperative transmission. Just the i th TX is shown, but in general multiple TXs can be used. At the source of information a binary information sequence χ of length $2SR_\chi$ is convolutionally encoded with code rate R_χ . After random interleaving and quadrature phase shift keying (QPSK) modulation with Gray labeling, the data symbols $b_i[m, n]$ are mapped on the OFDM time-frequency grid, where $m \in \mathcal{I}_M = \{0, \dots, M-1\}$ denotes the symbol time at rate $1/T_S$ and $n \in \mathcal{I}_N$ denotes the subcarrier index. This is done such that each block contains S coded data symbols $b_i[m, n] \forall [m, n] \in \mathcal{B}$, where \mathcal{B} denotes the two dimensional data symbol position index set in the time-frequency plane. For $[m, n] \notin \mathcal{B}$ we define $b[m, n] = 0$. Note that $b_i[m, n]$ also depends on the STC used.

In each data block J pilot symbols $p_i[m, n] \forall [m, n] \in \mathcal{P}$ are transmitted. The sets \mathcal{B} and \mathcal{P} are disjoint. For $[m, n] \notin \mathcal{P}$ we define $p_i[m, n] = 0$. The elements of the pilot symbols $p_i[m, n]$ for $[m, n] \in \mathcal{P}$ are randomly chosen from the QPSK symbol set $\{\pm 1 \pm j\}/\sqrt{2}$. To build the OFDM transmission block, the data symbols $b_i[m, n]$ and the pilot symbols $p_i[m, n]$ are added, giving

$$d_i[m, n] = b_i[m, n] + p_i[m, n]. \quad (1)$$

All indices not covered by \mathcal{B} and \mathcal{P} are used as guard band.

Subsequently, a N -point inverse discrete Fourier transform (IDFT) is carried out and the CP is inserted. An OFDM symbol, including the CP, has length $N + G$ chips at a chip rate of $1/T_C = (N + G)/T_S$. This signal is denoted by $x_i(k')$. To simulate non-sample-spaced timing offsets, we need to use the

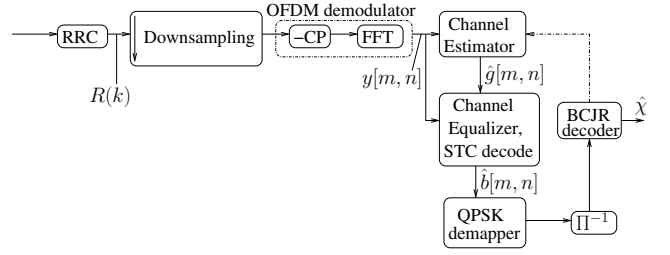


Fig. 3. Receiver model.

oversampled domain. Therefore, $x_i(k')$ is upsampled using an oversampling factor of $\Omega = 4$, obtaining $X_i(k)$.

To account for *timing errors and frequency offsets*, we introduce

$$X'_i(k) = X_i(k - \delta_i) \cdot e^{j2\pi f_{\text{off},i}k/R_O},$$

where $R_O = 1/T_O = \Omega R_C$ denotes the sampling rate of the oversampled signal. That is, we assume that the timing errors are an integer multiple of the *oversampled* chip time T_O and not just an integer multiple of T_C .

2) *Channel*: The channel impulse response is calculated using discrete convolutions as

$$H_i(k) = H_{\text{Tx},i}(k) * H_{\text{Ph},i}(k) * H_{\text{Rx}}(k), \quad (2)$$

containing the effects of the physical channel $H_{\text{Ph},i}(k)$, the root-raised cosine (RRC) filters at the TX side $H_{\text{Tx},i}(k)$ and the receiver side $H_{\text{Rx}}(k)$.

For the physical channel, we use a block-fading frequency selective channel model with a unit-power exponential power delay profile with 64 taps in the oversampled domain, having a RMS delay spread of 520 ns. Subsequently, the coefficients are weighted to represent the path loss of the individual links.

3) *Receiver*: The block model of the receiver is shown in Fig. 3. The received signal after downsampling, CP removal and DFT can be written as

$$y[m, n] = \sum_i g_i[m, n]d_i[m, n] + w[m, n], \quad (3)$$

where $w[m, n]$ denotes symmetric complex additive white Gaussian noise with zero mean and covariance σ_w^2 .

The frequency responses of the channels from the individual TXs, $g_i[m, n]$, include both the effects of the channels and of the timing errors and frequency offsets. Either the individual channels, $g_i[m, n]$, or the compound channel $g[m, n] = \sum_i g_i[m, n]$, is estimated making use of the previously inserted pilots. We consider two types of channel estimation: block-fading channel estimation and time-variant channel estimation. Both estimators will be described in Section IV.

We apply different equalizers to obtain the estimated received symbols as described below. Subsequently, the estimated symbols are demapped, deinterleaved and decoded. In the decoding process we use a BCJR decoder [11]. The decoding process can be further improved using an iterative implementation exploiting the soft output from the BCJR decoder to obtain a better estimation of the channel [12].

B. Space-time codes

We investigate the effect of delay and frequency offsets using two basic space-time codes, the Alamouti and the delay diversity STCs. Note that their combination with OFDM enable these codes to become delay tolerant.

1) *Delay diversity space-time code*: Multipath diversity, or equivalently, frequency diversity can be exploited in channels with time dispersion. It was shown that introducing artificial multipath diversity by transmitting the *same signal* from different antennas with an artificially introduced cyclic delay is advantageous [13].

Distributed cooperative transmission systems are suitable for this kind of STC since the delays from different nodes are distinct in general. The CP turns such delays into cyclic rotations of the OFDM symbol. This STC is completely transparent for the receiver, which simply observes the compound radio channel subject to additional frequency dispersion.

Channel equalization is done either by a zero-forcing equalizer:

$$\hat{b}_{\text{ZF}}[m, n] = \frac{y[m, n]\hat{g}[m, n]^*}{|\hat{g}[m, n]|^2}, \quad (4)$$

where \hat{g} is the estimate of the compound channel, or by the MMSE equalizer:

$$\hat{b}_{\text{MMSE}}[m, n] = \frac{y[m, n]\hat{g}[m, n]^*}{|\hat{g}[m, n]|^2 + \sigma_w^2}. \quad (5)$$

2) *Alamouti scheme*: The well-known Alamouti STC employs two transmit and one receive antennas [1] to exploit multi-antenna diversity at no rate loss. It must be noted that the Alamouti scheme was initially designed for block fading channels. For time variant channels, the receiver needs to be adjusted. We use a zero forcing implementation for time-variant Alamouti equalization as discussed in [14].

III. IMPACT OF TIMING ERRORS AND FREQUENCY OFFSETS

To analyze the impact of timing errors and frequency offsets of the multiple TXs we analyze their effect on the received signal before downsampling,

$$R(k) = \sum_{i=1}^I [X_i(k - \delta_i) e^{j2\pi f_{\text{off},i} k T_o}] * H_i(k) + W(k), \quad (6)$$

where I denotes the number of TXs and δ_i represents the sum of the timing errors of the i th TX and the propagation delay in the i th channel. By variable transform, one can show that this is equal to

$$R(k) = \sum_{i=1}^I \sum_{\ell} X_i(k - \ell) H_i(k, \ell - \delta_i) + W(k), \quad (7)$$

where

$$H_i(k, \ell) \doteq H_i(\ell) e^{j2\pi f_{\text{off},i} (k - \ell) T_o}$$

denotes the time-variant impulse response with delay time index ℓ . Hence, *both the delay and frequency offsets can be shifted into the effective channel $H_i(k, \ell)$* . Also note that due to the frequency offset, the effective channel becomes time

variant. This can be interpreted as a Doppler shift on each of the channels. Then, all signals sum up at the receiver.

To see the impact of the time variance on the frequency responses $g_i[m, n]$ in the signal model (3), we look at the channel for each OFDM symbol individually. Hence, the time variant channel affecting symbol m can be written as

$$\begin{aligned} H_i(m, k'', \ell) & \doteq H_i(m(N + G)\Omega + k'', \ell) \\ & = H_i(\ell) e^{j2\pi f_{\text{off},i} (k'' - \ell) T_o} \underbrace{e^{j2\pi f_{\text{off},i} (m(N + G)) T_o}}_{e^{jm\phi_i} \dots \text{phase rotation}} \\ & = H_i(k'', \ell) \cdot e^{jm\phi_i}, \end{aligned}$$

where k'' denotes the sample time index within the m th OFDM symbol. The phase offset $e^{jm\phi_i}$ only depends on the symbol index, therefore it can be treated as a constant for the convolution in (7).

We make use of (i) the fact that the CP ensures cyclical convolutions in (7), (ii) the assumption that the bandlimiting filters and the downsampling ($k \rightarrow k'$) remove all spectral contributions outside the bandwidth B . Using the discrete N -point Fourier transform of the channel, we obtain the time-variant channel frequency response

$$g_i(m, n, k'') \doteq \mathcal{F}_{(\ell)}^N \{H_i(k'', \ell - \delta_i)\} \cdot e^{jm\phi_i}.$$

Taking the assumption at the receiver that the frequency offset of the subchannels is small, hence $f_{\text{off},i} \ll B/N$ (i.e. we will not observe intercarrier interference), it can be shown that one can neglect the dependence on k'' , hence the effective channel becomes

$$g_i[m, n] = \mathcal{F}_{(\ell)}^N \{H_i(\ell - \delta_i)\} \cdot e^{jm\phi_i}. \quad (8)$$

This shows that carrier frequency offsets transform into a *complex rotation of the channels* for every OFDM symbol.

IV. CHANNEL ESTIMATION

The Alamouti and delay diversity STCs need different implementations of the channel estimation and equalization. For the *Alamouti STC*, we estimate the effective subchannels from each TX $g_i[m, n]$ individually, and consider the structure of the Alamouti code for equalization to decode the original symbols.

For the *delay diversity STC*, we estimate the compound channel $g[m, n] = \sum_i g_i[m, n]$, i.e. the superpositions of the *effective* channels from all TXs. There is no additional complexity in the channel equalization.

A. Block-fading channel estimation

Given the insights from Section III that frequency offsets can be interpreted as time variant channels, block-fading channel estimation is suboptimal. Since it is employed in many current communication systems, we include it just as a baseline performance metric.

For *delay diversity* we use least-squares (LS) channel estimation on the available pilot blocks (combined at the receiver) and average the estimates for each subcarrier.

TABLE I
SYSTEM PARAMETERS

Parameter	Symbol	Value
# of OFDM symbols in one block	M	12
# of frequencies	N	512
Cyclic prefix length	G	128 samples
Sampling rate	R_C	7.68 MHz
Sample time	T_C	130.21 ns
Oversampling factor	Ω	4
RRC roll-off factor	ρ	0.2
Convolutional code rate	R_x	1/2

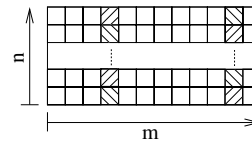


Fig. 4. Pilots are marked with diagonal lines. For the Alamouti scheme, orthogonal pilots are used (indicated by a different pattern), blank squares correspond to data subcarriers. The subcarriers with $n \notin \{106, \dots, 405\}$ are used as guard band.

For the *Alamouti STC* we need to estimate both channels independently. Hence, different pilot sequences are used for the two TXs, which are orthogonal in frequency [15]. In this way, the receiver uses LS channel estimation on the (orthogonal) pilots for each TX.

B. Time variant channel estimation

Due to the presence of *frequency offsets* in the distributed TXs, we require a *time variant* channel estimator, even for scenarios with *block fading* channels.

For delay diversity all TXs use the same pilot pattern. The time-variant frequency-selective channel estimator is based on discrete prolate spheroidal sequences (DPSs) that are used in the time -and frequency- domain. A DPS subspace projection in the *time and frequency* domain was used in [16]. A joint time-frequency iterative solution is discussed in [12] building on iterative soft-symbol feedback presented in [17]. Note that in Fig. 3 the soft output information from the BCJR decoder can be used iteratively to obtain a better channel estimation. The channel estimation is performed using the minimum mean squared error filter as described in [12, (4)], using extrinsic soft symbol feedback from the BCJR decoder.

For the Alamouti STC we use pilot sequences that are orthogonal in frequency [15], at each TX. Each of the channels is estimated independently exploiting a time variant channel estimator based on DPSs like in the case of delay diversity.

V. SIMULATIONS

A. System configuration

We consider a distributed cooperative scenario with two TXs. The configuration of the OFDM system simulated is similar to LTE in the uplink (see Table I). The pilot positions are shown in Fig. 4.

For the Alamouti scheme, in each subcarrier n , the Alamouti code is used on two consecutive OFDM symbols (skipping pilots), hence $[m_1, m_2] \in \{[1, 2], [3, 5], [6, 7], [8, 9], [10, 12]\}$, where $[m_1, m_2]$ denote the indices of the first and second symbol used for the Alamouti code.

Note that the path loss and large scale fading of the frequency-selective channels are different, reflecting the fact that the TXs are spatially distributed. We let the effective path loss of the two channels be $L_1 = 95.45$ dB and $L_2 = 90.70$ dB.

B. Simulation results

We simulated the system performance in terms of the BER over different levels of receive signal-to-noise ratio (SNR). The SNR is defined as the ratio of the average sum received power and the noise power.

First, we investigate the effects of frequency offsets at the TXs. Fig. 5 shows the BER as a function of the frequency offset of TX 1 relative to the receiver, while the frequency offset of TX 2 is fixed to -250 Hz. As discussed, even with block-fading physical channels, time-variant channel estimation is necessary to combat the time variations in the effective channel introduced by the frequency offsets. With time-variant channel estimation the system performance is stable, for a wide range of frequency offsets.

We observe that in general the results with Alamouti STC outperform the ones of delay diversity, particularly at high SNR. This is due to the combination of the different types of channel estimation used for the delay diversity and the Alamouti STCs, and the pilot pattern. For Alamouti, the channels from the TXs are estimated and tracked independently. Since each channel has its individual frequency shift, the time variation of each subcarrier can be easily interpolated. For delay diversity, the compound channel, including a superposition of two frequency offsets must be estimated at the receiver, which is not supported by the pilot pattern.

For block fading channel estimation, we can observe an interesting effect: the delay diversity STC has its minimum BER around $f_{\text{off},1} = -250$ Hz, while for the Alamouti STC the minimum is at 0 Hz. This is due to the different types of codes. When in the Alamouti scheme one of the TXs has no frequency offset, these symbols may be decoded correctly from that TX, which improves the overall performance of the scheme.

Investigating the impact of timing offsets, we change the relative delay of TX 2, while TX 1 has perfect timing synchronization with the receiver. Fig. 6 presents the BER as a function of the relative delay from TX 2, given in number of samples. By oversampling, we also consider fractional delay offsets. Note that the CP of the considered system is 128 samples.

The results in Fig. 6 show that OFDM is robust to delay offsets due to the CP. Small timing offsets transform into a cyclic rotation of the OFDM symbol, which is compensated by proper channel estimation. The performance deteriorates when the delay offset plus the impulse response length of the channel exceed the CP. In our case, the channel impulse

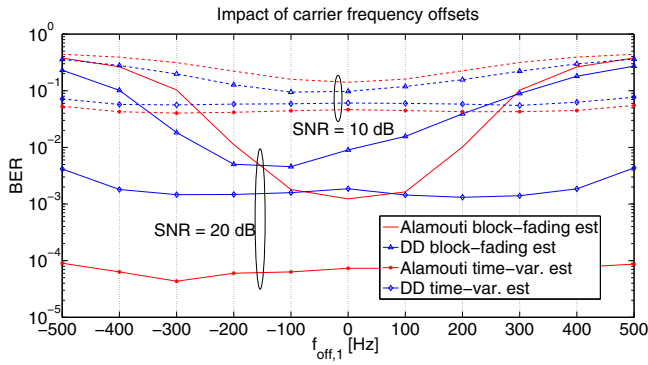


Fig. 5. BER performance of distributed Alamouti and delay diversity STC under different frequency offsets of the nodes. $f_{off,2} = -250$ Hz.

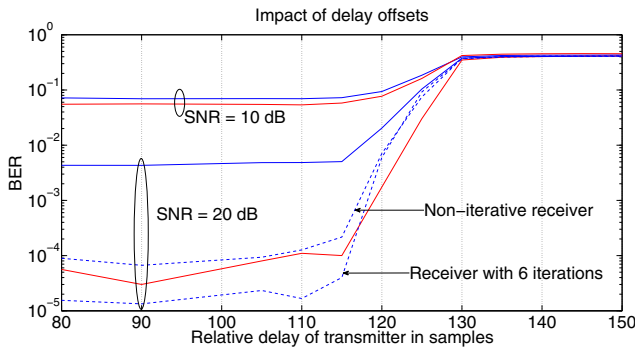


Fig. 6. BER of distributed Alamouti (red lines) and delay diversity (blue lines) STCs under different timing errors using a time-variant channel estimator with $f_{off,1} = -250$ Hz, $f_{off,2} = 500$ Hz. Continuous lines correspond to a zero-forcing equalizer, dashed lines correspond to the MMSE equalizer.

response has a length of 16 samples, so relative delay offsets of up to 112 samples can be tolerated, which is also reflected by our simulations.

In Fig. 5, we considered a relative delay of 60 samples. The CP compensated the effect of the overall relative delay in the system regardless of frequency offsets. Similarly, in Fig. 6, different nodes frequency offsets, $f_{off,1} = -250$ Hz and $f_{off,2} = 500$ Hz, were considered. Time-variant channel estimation is able to compensate for these regardless of the relative delays.

As shown in Fig. 6 the BER obtained with a MMSE equalizer is significantly lower than the one obtained with a zero-forcing equalizer. Further improvements can be achieved using multiple iterations at the receiver. Overall, more than 2 orders of magnitude are achieved combining a MMSE equalizer with an iterative channel estimator at the receiver.

In Fig. 5, the curves obtained using a MMSE equalizer at the receiver are not shown since the simulation BER was lower than 10^{-5} for $-400\text{Hz} \leq f_{off,1} \leq 400\text{Hz}$.

VI. CONCLUSIONS

Cooperative communications is a promising technology to increase the reliability of the link and the data rate. However, different carrier frequency offsets and timing errors from the individual nodes provide a challenge to this technology.

Individual carrier frequency offsets lead to a strongly time-variant compound channel (even if each individual physical channel is static). Timing offsets may lead to the misalignment of the space-time code used.

We solved both problems by combining STCs with OFDM and time-variant channel estimation. The OFDM CP turns the timing offset into a cyclic rotation of the OFDM symbol, while time-variant channel estimation takes care of the channel variability due to frequency offsets. By this system design, we improved the BER performance by an order of magnitude.

REFERENCES

- [1] S. Alamouti, "A simple transmit diversity technique for wireless communications," *IEEE Journal on Selected Areas in Communications*, vol. 16, no. 8, pp. 1451–1458, 1998.
- [2] E. Viterbo, Y. Hong, and A. Grant, "Timing errors in distributed space-time communications," in *Proc. Australian communications theory workshop*, pp. 70–75.
- [3] M. Damen and J. A. Hammons, "Delay-tolerant distributed-TAST codes for cooperative diversity," *IEEE Transactions on Information Theory*, vol. 53, no. 10, Oct. 2007.
- [4] M. Sarkiss, M. O. Damen, and J.-C. Belfiore, "2 x 2 delay-tolerant distributed space-time codes with non-vanishing determinants," in *IEEE PIMRC 2008*, 2008.
- [5] Y. Li and X. Xia, "A family of distributed space-time trellis codes with asynchronous cooperative diversity," *IEEE Transactions on Communications*, vol. 55, pp. 790–800, 2007.
- [6] A. R. Hammons and H. E. Gamal, "On the theory of space-time codes for PSK modulation," *IEEE Transactions on Information Theory*, vol. 46, no. 2, pp. 524–542, Mar. 2000.
- [7] "3rd Generation Partnership Project; Technical Specification Group Radio Access Network; Evolved Universal Terrestrial Radio Access (E-UTRA); LTE Physical Layer - General Description," 2009.
- [8] "802.11-2007, IEEE Standard for Information Technology-Telecommunications and Information Exchange Between Systems-Local and Metropolitan Area Networks-Specific Requirements - Part 11: Wireless LAN Medium Access Control (MAC) and Physical Layer (PHY) Specifications," 2008.
- [9] "ETSI Standard: EN 300 744 V1.5.1, Digital Video Broadcasting (DVB); Framing structure, channel coding and modulation for digital terrestrial television," 2004.
- [10] S. B. Weinstein and P. M. Ebert, "Data transmission by frequency-division multiplexing using the discrete fourier transform," vol. 19, no. 5, pp. 628–634, October 1971.
- [11] L. Bahl, J. Cocke, F. Jelinek, and J. Raviv, "Optimal decoding of linear codes for minimizing symbol error rate," *IEEE Transactions on Information Theory*, vol. IT-20(2), no. 2, pp. 284–287, Mar. 1974.
- [12] S. Rossi and R. Müller, "Slepian-based two-dimensional estimation of time-frequency variant MIMO-OFDM channels," *IEEE Signal Processing Letters*, vol. 15, pp. 21–24, 2008.
- [13] N. Seshadri and J. H. Winters, "Two signaling schemes for improving the error performance of frequency-division-duplex (FDD) transmission systems using transmitter antenna diversity," *Vehicular Technology Conference, 1993 IEEE 43rd*, pp. 508 – 511, May 18–20, 1993, secacucus, NJ, USA.
- [14] A. Vielmon, Y. Li, and J. Barry, "Performance of Alamouti transmit diversity over time-varying rayleigh-fading channels," *Wireless Communications, IEEE Transactions on*, vol. 3, no. 5, pp. 1369 – 1373, Sept. 2004.
- [15] H. Minn and N. Al-Dhahir, "Optimal training signals for MIMO OFDM channel estimation," *IEEE Transactions on Wireless Communications*, vol. 5, no. 5, pp. 1158–1168, May 2006.
- [16] T. Zemen, H. Hofstetter, and G. Steinböck, "Successive Slepian subspace projection in time and frequency for time-variant channel estimation," in *14th IST Mobile and Wireless Communication Summit (IST SUMMIT)*, Dresden, Germany, June 19-22 2005.
- [17] T. Zemen, C. F. Mecklenbräuker, J. Wehinger, and R. R. Müller, "Iterative joint time-variant channel estimation and multi-user detection for MC-CDMA," vol. 5, no. 6, pp. 1469–1478, June 2006.